EPJ Web of Conferences **75**, 03006 (2014)
DOI: 10.1051/epjconf/ 20147503006

Structural and Electromagnetic Properties of Ni-Mn-Ga Thin Films Deposited on Si Substrates

M. J. Pereira[1,a], A. A. C. S. Lourenço[1], V. S. Amaral[1]

[1]Department of Physics and CICECO, University of Aveiro, 3810-193 Aveiro, Portugal

Abstract. Ni_2MnGa thin films raise great interest due to their properties, which provide them with strong potential for technological applications. Ni_2MnGa thin films were prepared by r.f. sputtering deposition on Si substrates at low temperature (400 ºC). Film thicknesses in the range 10-120 nm were obtained. A study of the structural, magnetic and electrical properties of the films is presented. We find that the deposited films show some degree of crystallinity, with coexisting cubic and tetragonal structural phases, the first one being preponderant over the latter, particularly in the thinner films. The films possess soft magnetic properties and their coercivity is thickness dependent in the range 15-200 Oe at 300K. Electrical resistivity measurements signal the structural transition and suggest the occurrence of avalanche and return-point memory effects, in temperature cycling through the magnetic/structural transition range.

1 Introduction

The Ni-Mn-Ga alloy belongs to the class of Heusler alloys that undergo a structural (martensitic) transition involving a transformation in both structural and magnetic properties of the material [1]. This shape memory alloy has become very popular because of its reversible strain induced by a magnetic field [2], a concept called magnetostrain, which was first reported by Ullakko et al. in 1996 [3]. The magnetostrain presented by Ni-Mn-Ga can go up to 10% and originates from twin boundary motion [1]. Despite the interesting properties that make Ni-Mn-Ga such a popular material, the brittleness of this alloy in the bulk form constitutes a relevant limitation for its use in practical applications. This is one of the reasons that make the study of Ni-Mn-Ga thin films, which are more ductile than the bulk material, extremely relevant. Adding to this, producing this material in the form of thin films allows its application to the development of micro and nano electro-mechanical systems [4-5]. Most of the research performed so far on the Ni-Mn-Ga system material was focused on the bulk material and only recently some work on Ni-Mn-Ga thin films has been developed. One of the most interesting aspects of the study of Ni-Mn-Ga thin films is the investigation of the role of the substrate in the film's structure and thus in the resulting film properties. Also, the parameters established for the deposition technique are of great relevance for obtaining the desired material properties, as these properties are strongly dependent on the film's composition [6]. Here we investigate the electromagnetic properties of Ni-Mn-Ga films with several thicknesses deposited by radio-frequency (RF) magnetron sputtering onto $Si(100)/SiO_2$ substrates.

2 Experimental Details

Ni-Mn-Ga thin films were deposited onto $Si(100)/SiO_2$ substrates by radio-frequency (RF) magnetron sputtering. The deposition of the films took place at a substrate temperature of about 400 ^{0}C in an argon atmosphere of less than 10-2 mbar. These conditions are similar to the ones used in [7]. The deposited films possess thicknesses from 10 nm to 120 nm. The films' thicknesses were obtained through XRR (X-ray reflectivity) and SEM/TEM measurements. The X-ray diffraction measurements were performed on a PANalytical X'Pert PRO MRD X-ray diffraction instrument with a Cu-Kα radiation source. Isothermal magnetization loops were performed in a Cryogenics VSM (Vibrating Sample Magnetometer) equipment with a resolution of $5x10^{-5}$ emu, whereas magnetization as a function of temperature measurements were performed in a Quantum Design SQUID (Superconducting Quantum Interference Device) magnetometer. The magnetic field was applied in the plane of the films. The chemical composition of the samples was determined by EDS (Energy-dispersive X-ray Spectroscopy). Electrical resistivity measurements were performed with a homemade four probe resistivity measurement system.

[a] Corresponding author: mariasapereira@ua.pt

3 Results and Discussion

Fig. 1 shows the XRD scans of some of the thinner films, namely the ones with thicknesses of 10 nm, 15 nm and 60 nm, performed at room temperature using grazing incidence configuration in order to suppress the substrate contribution, since these films are quite thin. Fig. 2 shows the XRD scans in the θ-2θ geometry, performed at room temperature, of the Ni-Mn-Ga films with thicknesses of 20 nm, 40 nm and 80 nm.

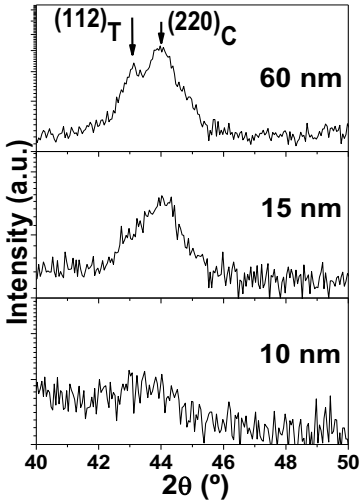

Figure 1. Grazing incidence XRD diffractograms for samples with thicknesses of 10 nm, 15 nm and 10 nm.

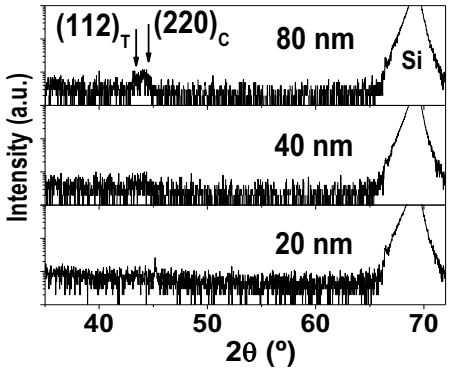

Figure 2. XRD diffractograms for samples with thicknesses of 20 nm, 40 nm and 80 nm.

In fig. 1 it is possible to see that for the 10 nm film there is almost no noticeable presence of the tetragonal (martensitic) phase and only a contribution from the cubic (austenitic) phase can be perceived. For the 15 nm film we notice a subtle contribution from the tetragonal coexisting with the cubic phase. The presence of the tetragonal phase becomes even more evident for the 60 nm film. Fig. 2 confirms the increasing contribution of the tetragonal phase as the film thickness increases. For the 120 nm film both phases seem to contribute equally for the film's structure. The presence of the SiO_2 layer between the substrate and the film has been found to promote the growth of the cubic structure [8]. Fig. 3 a) and c) show surface SEM images of the 120 and 80 nm films, respectively. Fig. 3 b) and d) show cross section SEM images of the 120 and 80 nm films, respectively. Fig. 3 e) shows a cross section TEM image of the 60 nm film.

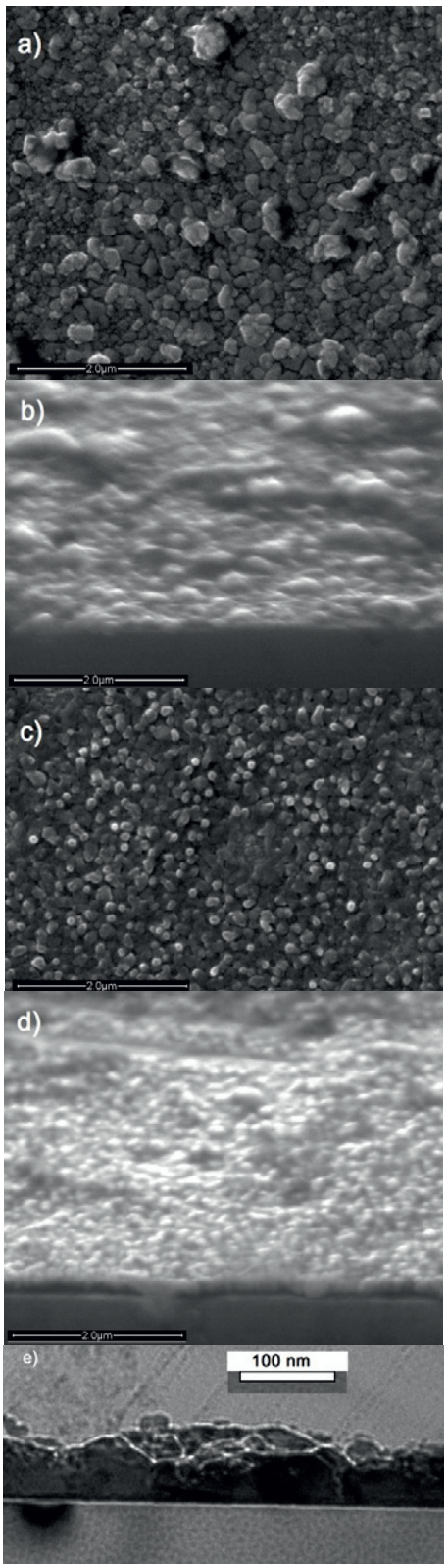

Figure 3. SEM and TEM images: a) b) 80 nm sample, c) d) 120 nm sample and e) 60 nm sample.

We can see that the 80 nm and 120 nm samples have an estimated grain size of 0.36 μm and 0.2 μm, respectively. This estimation of the grain size provides information on the roughness and homogeneity of the films' surfaces. For instance, since the 80 nm film shows bigger grains on its surface than the 120 nm film, the former is thus expected to possess a higher degree of roughness than the latter. The cross-section image of the 60 nm film clearly shows the Si substrate, the SiO_2 intermediate layer with a thickness of about 5 nm and the film with a surface roughness of about 20 nm.

Fig. 4 shows the hysteretic curves of magnetization as a function of the applied magnetic field taken at 300 K for the films with thicknesses of 20 nm, 40 nm and 80 nm. The analysis of these curves show that at 300 K the films exhibit soft magnetic properties characterized by narrow hysteresis, low coerciviy and high magnetic saturation values. The saturation magnetization (M_S) and coercivity (H_C) values obtained for some of the films are listed on Table 1. MS values at 300 K range from 30 to 200 emu/cm^3. No clear dependence can be established between these values and film thickness. Coercivity (H_c) values range from 15 to 200 Oe, which can be considered within the same order of magnitude of that of bulk alloys [9]. Fig. 5 shows the coercivity values of the deposited films as a function of film thickness at 300K. As it can be seen, there is an increase of Hc with thickness, with a clear step between 60-80 nm. This further rise may be correlated with the increase of tetragonal phase in the films thicker than 60 nm. The temperature dependence of the films' magnetization with applied fields of 50, 100 and 2000 Oe was investigated for the samples with thicknesses of 60, 80 and 120 nm in the range of 5 K to 380 K.

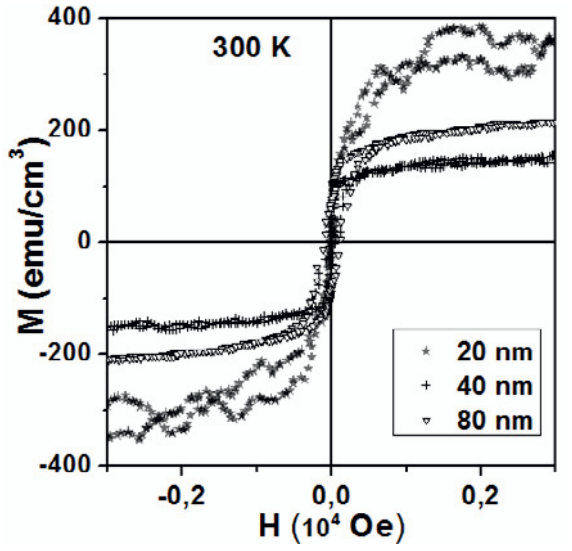

Figure 4. Magnetization as a function of the applied magnetic field taken at 300 K for the films with thicknesses of 20 nm, 40 nm and 80 nm.

Fig. 6 shows the corresponding curve obtained for the 60 nm film, which is representative of the behavior of the analyzed films. The 60 nm sample displays a T_C of approximately 350 K, obtained by the extremal derivative dM/dT. No evidence of first-order structural martensitic to austenitic transition was detected, since no sudden rise in magnetization is noticeable in the temperature range contemplated by the any of the magnetization vs temperature measurements performed. This absence of structural transition evidence may mean that the change in magnetization during the structural transition is too small to be detected in these measurements. The Curie temperature (T_C) of the films increases with increasing Ni content (Table 2), as expected [6].

Table 1. Magnetization saturation and coercivity values at 300K for the several film thicknesses.

Temperature (K)	t (nm)	M_S (emu/cm^3)	H_C (Oe)
300 K	20	300	15
	30	30	-
	40	175	50
	60	150	70
	80	200	150
	120	110	200

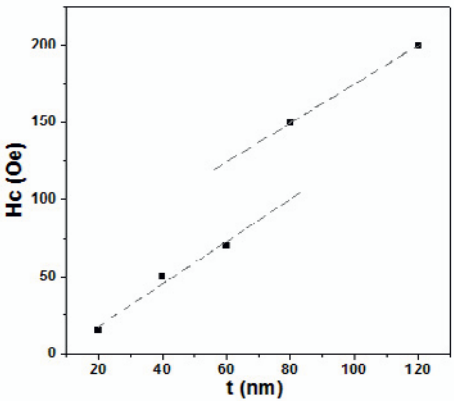

Figure 5. Coercivity values plotted as a function of film thickness.

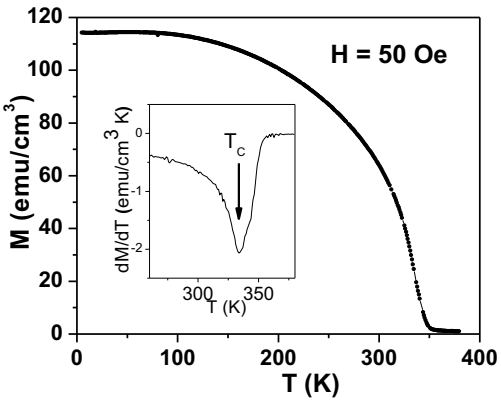

Figure 6. Magnetization versus temperature and corresponding first derivative for the 60 nm sample.

Table 2. Film composition and T_C values for samples with thicknesses of 60, 80 and 120 nm.

t (nm)	Ni content (%)	Mn content (%)	Ga content (%)	T_C (K)
60	59	27	14	340
80	53	20	27	316
120	56	19	26	330

Electrical resistance measurements were performed, with particular focus on the transition temperature range. Fig. 7 shows a characteristic resistance versus temperature cycle, 300K to 370K. The jumps appearing at about 340K and 330K in heating and in cooling respectively, seem to signal the first-order martensitic transformation temperatures. The hysteretic behavior shown by the resistance is typical of shape memory alloys thin films around the martensitic transformation temperature [6]. The structural transition seems to have here, on the dependence of resistance on temperature, a much more pronounced effect than in the magnetization measurements. It is also found that the limits of the temperature cycling modify the smaller details of the curves, suggesting the occurrence of avalanche and return-point memory effects, which will be discussed elsewhere.

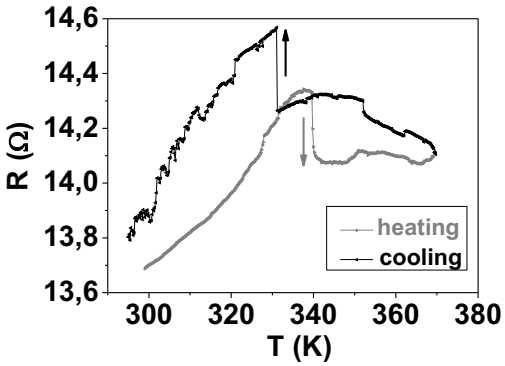

Figure 7. Resistance versus temperature for the 60 nm sample.

4 Conclusions

The studied films show the coexistence of both cubic and tetragonal phases. The cubic phase is preponderant over the tetragonal phase for films with lower thickness values (~ 10 nm to 60 nm) but there is a clear increase of tetragonal phase with film thickness. The films possess ferromagnetic behavior at room temperature and they exhibit soft magnetic properties. Coercivity increases with film thickness. The magnetic transition is clearly observed only in curves of magnetization as a function of temperature. The structural transition has a visible impact on the electrical resistivity changes as a function of temperature on cycling the temperature. These measurements seem to suggest the occurrence of avalanche and return-point memory effects, which are currently under study.

5 Acknowledgements

The work is supported by the program COMPETE/ FFEDER and FCT under projects PTDC/CTM-NAN/115125/2009 and CICECO - PEst-C/CTM/LA0011/2013. M.J. P acknowledges her research grant from FCT project.

References

1. A. Planes, L. Mañosa, M. Acet, J. Phys. Condens. Matter **21**, 233201 (2009)
2. M. Chmielus, X. X. Zhang, C. Witherspoon, D. C. Dunand, P. Müllner, Nature Materials **8**, 863-866 (2009)
3. K. Ullakko, J. K. Huang, C. Kantner, R. C. O'Handley, V. V. Kokorin, Appl. Phys. Lett. **69**, 1966 (1996)
4. A. Annadurai, A. K. Nandakumar, S. Jayakumar, M. D. Kannan, M. Manivel Raja, S. Bysak, R. Gopalan, V. Chandrasekaran, J. Magn. Magn. Mater. **321**, 630-634 (2009)
5. M. Thomas, O. Heczko, J. Buschbeck, U. K. Rößler, J. McCord, N. Scheerbaum, L. Schultz, S. Fähler, New J. of Phys. **10**, 023040 (2008)
6. V.V. Khovaylo, V.D. Buchelnikov, R. Kainuma, V.V. Koledov, M. Ohtsuka, V.G. Shavrov, T. Takagi, S.V. Taskaev, A.N. Vasiliev, Phys. Rev. B **72**, 224408 (2005)
7. M.Y. Teferi et al., Journal of Magnetism and Magnetic Materials **324**, 1882–1886 (2012)
8. A. C. Lourenço, F. Figueiras, S. Das, J. S. Amaral, G. N. Kakazei, D. V. Karpinsky, N. Soares, M. Peres, M. J. Pereira, P. B. Tavares, N. Sobolev, V. Amaral, N. M. Santos and A. L. Kholkin, MRS Proceedings **1250**-G08-02(2010)
9. I. Babita, R. Gopalan, M. Manivel Raja, V. Chandrasekaran, S. Ram, J. Appl. Phys. **102**, 013906 (2007)